Journal of Materials, Processing and Design (2023)
Clausius Scientific Press, Canada

DOI: 10.23977/jmpd.2023.070203
ISSN 2516-0923 Vol. 7 Num. 2

Synthesis, crystal structures and physicochemical performance of the triethylamine salt and copper (II) complex based on 3, 5-dinitropyrazole

Wei Du[1,2,a], Qing Ma[2,b], Ming Duan[1,c,*], Shaohua Gou[1,d,*]

[1]College of Chemistry and Chemical Engineering, Southwest Petroleum University, Chengdu, 100081, China
[2]Institute of Chemical Materials, CAEP, Mianyang, 621999, China
[a]1565524886@qq.com, [b]qingma@caep.cn, [c]mduan@swpu.edu.cn, [d]591570164@qq.com
**Corresponding author*

Keywords: Energetic ionic salts, Energetic coordination compound, X-ray diffraction, Physicochemical properties

Abstract: Two novel energetic ionic and coordination frameworks based on 3, 5-dinitropyrazole (3, 5-DNP) were prepared under the facile reaction conditions. They were characterized by FT-IR spectroscopy, Raman spectrum, single-crystal X-ray analysis and differential scanning calorimetry thermal analysis (DSC). Hirshfeld analysis showed that they both presented strong hydrogen-bond intermolecular interactions. Thermal properties and the nonisothermal thermokinetic parameters were obtained by differential scanning calorimeter (DSC) as well as Kissinger, Ozawa and Starink methods. The two energetic materials exhibit excellent thermal stabilities ([DNP] NH $(Et)_3$: T_m=251℃, T_d=377℃; Cu $[DNP]_2[H_2O]_2$: T_d=350℃). They can be potential candidates for heat-resistant energetic materials for military uses.

1. Introduction

Developing different forms of energetic materials (EMs) has become a fascinating research area in recent years, not being limited in neutral organic compounds. Among them, ionic salts and coordination compounds (including metal-organic frameworks) are the hotspot materials in the investigations of EMs and they behave significant and special physicochemical performance than other neutral compounds in most cases. [1,2]

Azole-based energetic ionic materials are always a fascinating calls of multi-nitrogen frameworks, which contain multiple N-N, C-N chemical bonds and stable electrovalent bond depositing sufficient energy. Since 2010, many energetic ionic compounds grounding on pyrazole were massively prepared, which were mainly consist of 3,4,5-trinitropyrazole (3,4,5-TNP)-, [3,4] 3,4,5-trinitropyrazole-1-ol (TNPO)-, [5] 4-amino-3,5-dinitropyrazole (ADNP)- , 4-nitramino-3, 5-dinitropyrazole (4-NADNP)- and 1-nitramino-3,5-dinitropyrazole (1-NADNP)-based organic salts. [6] Recently, metal ions were introduced into ADNP and 3,5-DNP, including K^+, Na^+, Li^+, Au^+, Cu^{2+}, Pb^{2+}, Sr^{2+}, Ba^{2+}, etc.[7,8] However, Drukenmüller et al supposed that salts of 3,5-DNP did not

tend to form single crystals in experiments. [7]

In the present work, two novel energetic materials based on 3, 5-dinitropyrazole (3, 5-DNP) were synthesized and their single crystals were also cultivated with structure confirmed by X-ray diffraction. Moreover, their intermolecular interactions were further investigated by the Hirshfeld-Surface analysis and the thermal performance were evaluated by non-isothermal kinetic methods.

2. Experimental Section

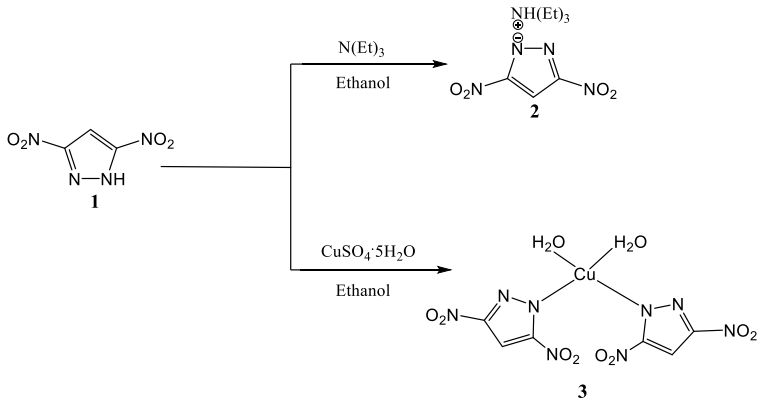

Scheme 1: Synthesis of two 3, 5-DNP based energetic materials.

2.1 Synthesis of 3, 5-dinitropyrazole (1):

3,5-dinitropyrazole was synthesized referred to the literature[9] and slightly improved in this work. 1,3-dinitropyrazole (1g, 6.3mmol) was dissolved in anisole (25mL) instead of benzonitrile (since the latter one is very toxic), and then heated to 147 ℃ for reaction in another 21 h. Subsequently, the anisole was evaporated and the left mixture was washed using little n-hexane. Then the crude product was recrystallized from benzene or toluene, and pale yellow solid were obtained (0.51g, yield 51%). DSC (5℃/min): 172 ℃ (m.p.), 333℃ (dec.) (lit.[12] m.p. 174-175℃). ^{1}H NMR (400 MHz, Acetone-d_6): 7.75 (1H, s). ^{13}C NMR (400 MHz, Acetone -d_6): 152.38, 100.08. Elemental analysis calcd for $C_3H_2N_4O_4$ (%) C 22.80, H 1.28, N 35.44, found C 22.62, H 1.33, N 35.40.

2.2 Synthesis of [DNP] NH (Et)3 (2):

3,5-dinitropyrazole (3,5-DNP) (0.158g, 1mmol) was dissolved in anhydrous ethanol (10 ml), then triethylamine (1 mmol) was added. The synthesis route is shown in Scheme 1. Then the mixture was stirring until clear and then filtered, the solution was left for evaporation in 5 days. The yellow crystal sheets were obtained (0.202g, yield 77.9%). DSC (5℃/min): 249 ℃ (m.p.), 377℃ (dec.). IR (KBr, cm^{-1}): γ=3443 (m), 3009 (m), 2817 (w), 2683 (m), 2504 (m), 1537 (s), 1474 (s), 1358 (s), 1148 (w), 1007 (w), 822 (w), 745 (w); Raman (cm^{-1}): ν=3316, 3130, 3054, 2292, 1461, 1403, 1231. ^{1}H NMR (400 MHz, DMSO-d_6): 7.27 (1H, s), 3.08 (9H, q), 2.47 (6H, s). ^{13}C NMR (400 MHz, DMSO-d_6): 156.85, 98.75, 46.23, 9.08. Elemental analysis calcd for $C_9H_{17}N_5O_4$ (%) C 41.69, H 6.61, N 27.01, found C 41.85, H 6.58, N 27.32.

2.3 Synthesis of Cu [DNP] 2[H2O]2 (3):

3,5-dinitropyrazole (3,5-DNP) (0.158g, 1mmol) was dissolved in anhydrous ethanol (10 ml),

then copper (II) sulfate pentahydrate (0.274 g, 1.1 mmol) was added to the above solution in a intense stirring. Then the precipitate was filtered, and the solution was left for evaporation in 24 hours. Several blue crystals appeared in the solution. Then the product were filtered and obtained (0.314g, yield 75.6%). DSC (5℃/min): 347℃ (dec.). IR (KBr, cm^{-1}): γ=3386(m), 3341(m), 3149(s), 1614(w), 1550(s), 1493(s), 1448(s), 1358(s), 1327(s), 1275(m), 1192(w), 1032(m), 994(m), 828(m), 744(m), 712(w); Raman (cm^{-1}): ν=3443, 3373, 3322, 1736, 1595, 1537, 1474, 1390, 1307, 1205, 1039, 719. Elemental analysis calcd for $C_6H_6CuN_8O_{10}$ (%) C 17.42, H 1.46, N 27.09, found C 17.35, H 1.51, N 27.14.

3. Results and discussion

3.1 X-ray diffraction crystallography

Crystals of compound 2 and 3 were obtained using slow evaporation of ethanol for 24 h in the room temperature(CCDC number： 1452000 and 1452001). All crystal parameters including bond lengths, bond angles, torsion angles and other relative data can be found in the Supporting Information. The optical microscopies of 2 and 3 are captured in Figure 1, which present the different appearance of the two compounds in sheets or blocks.

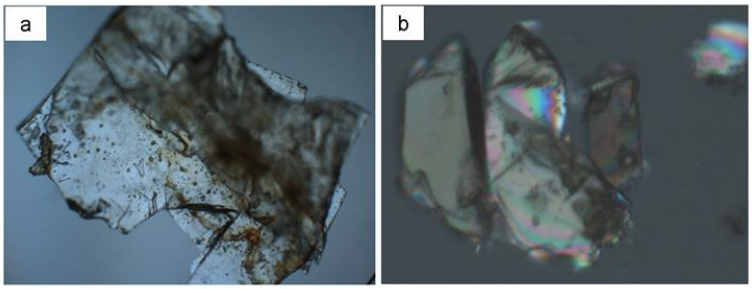

Figure 1: Optical microscopies of $[DNP]NH(Et)_3$ (a) and Cu $[DNP]_2[H_2O]_2$ (b) grown from slow evaporation in a ethanol solution.

As shown in Figure 2a, compound 2 contains one crystallographically independent anion and cation. The geometric structure of anion is the same with those of the units in compound 3. Due to the hydrogen bonding and electrovalent bonding, the nitrogen atoms between triethylamine and 3,5-DNP in compound 2 can form the stable molecular structure. The torsion angles suggesting that the two nitro groups are coplanar with the pyrazole ring. Figure 3a shows the crystal structure of coordination compound 3. For 3, the coplanar characteristics also exist. This indicates that the structures between copper and each 3,5-DNP molecule are nearly symmetrical. Comparing with 3,5-dinitropyrazole (1.430 and 1.452 Å)[9], the bond length of C-NO_2 in compound 2 and compound 3 are little different, which are 1.427 and 1.447 Å in compound 2 as well as 1.430 and 1.450 Å in compound 3.

The crystal packing of 2 and 3 are shown in Figure 2b and Figure 3b, 3c. It can be described as a layered arrangement in compound 2, and a similar like metal-organic framework (MOF) structure for compound 3 while along the (100) crystal-facet.

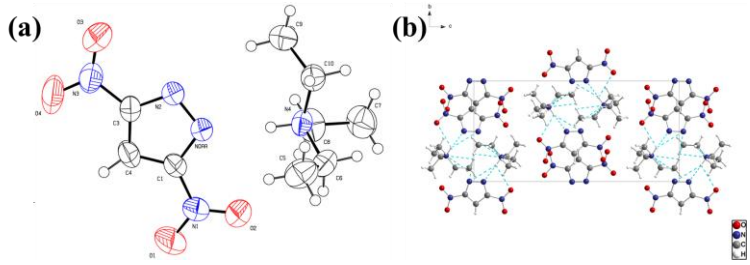

Figure 2: (a) Thermal ellipsoid plot (50%) and labeling scheme for 2. (b) Ball-and-stick packing diagram of 2 viewed down a axis. Dashed line indicates the strong intermolecular.

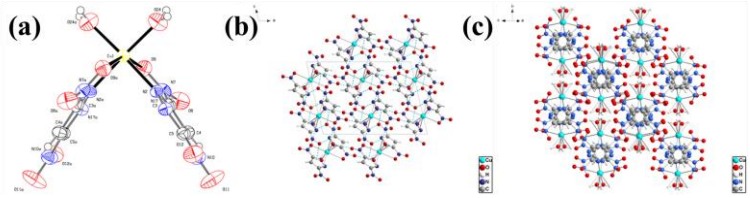

Figure 3. (a) Thermal ellipsoid plot (50%) and labeling scheme for 3. (b) 2×2×2 crystal packing viewed down the b axis. Dashed line indicates the strong intermolecular. (c) Ball-and-stick packing frameworks of 3 along the (100) facet.

3.2 Structure description

The sum of molecular interactions in compound 2 and 3 are depicted in fingerprint plots and their contributions for intermolcular close contacts are also summerized in Figure 4. The similarity of the two compounds is that the O ··H and H ··O close contacts are dominating interaction in the crystal packing, H ··H contacts of 2 are more than those of 3 while O ··O contacts of 2 are less than those of 3. However, the hydrogen-bond (HB) interactions are distinct in the two crystals. In compound 2, triethylamine cations provide more H atoms which can form sufficient HB interactions. But in compound 3, the HB interactions are mostly from the two H_2O molecules and O ··O contacts can attribute to the nitro groups from two DNP molecules. Meanwhile, the distributions of Cu ··N and Cu ··O contacts in 3 are close to those of C ··H and H ··C contacts.

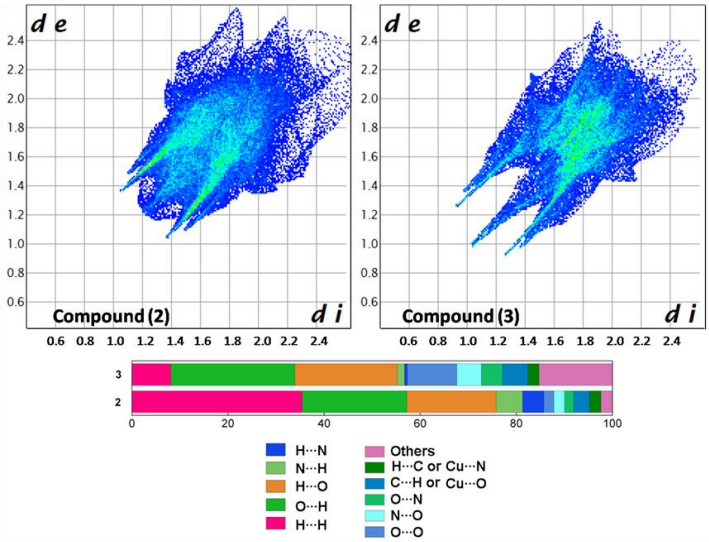

Figure 4: Fingerprint plots of 2 and 3 and their relative contributions to the Hirshfeld surface for intermolecular close contacts.

3.3 Vibrational analysis

The IR and Raman spectra of $[DNP]NH(Et)_3$ (2) and Cu $[DNP]_2[H_2O]_2$ (3) are shown in the Figure 5a, 5b. It is worthy of noting that IR spectra of compound 2 are dorminated by the C-H stretching bands at around 2500-3000 cm^{-1} and N-H stretching bands at 3000-3500 cm^{-1} while those of compound 3 are taken up by the O-H stretching bands at 3100-3400 cm^{-1}. 1200-1500 cm^{-1} belong to the nitro groups. For compound 2, the stretching modes of the $(C\text{-}N)_{ring}$ and $(N\text{-}N)_{ring}$ are observed as peaks of low intensity at $\gamma\approx1007$, 1358, 1474 and 1537 cm^{-1} (IR). For compound 3, the stretching modes of the $(C\text{-}N)_{ring}$ and $(N\text{-}N)_{ring}$ are observed as peaks of low intensity at $\gamma\approx1032$, 1448, 1493 and 1550 cm^{-1} (IR), which are basically in agreement with the results from Raman spectrum. Evidently, the energetic salt 2 and the coordination compound 3 show similar vibration bands between 1200 and 1500 cm^{-1} both in IR and Raman spectrums.

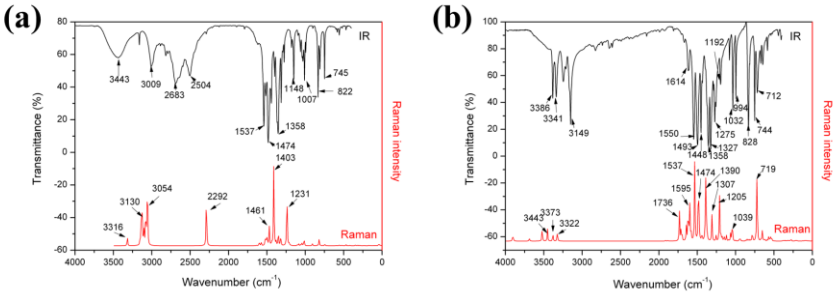

Figure 5: IR and Raman spectra of $[DNP]NH(Et)_3$ (a) and Cu $[DNP]_2[H_2O]_2$ (b).

3.4 Thermal behaviors and non-isothermal kinetics performance

Thermal behaviors concern about the stability of an energetic material. The thermal stabilities of two compounds were determined by differential scanning calorimetry (DSC) at different heating rates of 5, 10, 15, 20 K min^{-1} in Aluminum pans. Figure 6a, 6b shows that 2 melts at 249 ℃ (peak maxima) and decomposes at 377 ℃ (peak maxima) while 3 decomposes at 347 ℃ (peak maxima) at the heating rate of 5 K min^{-1}, which are both higher than those of RDX (T_m=205 ℃, T_d=210 ℃).

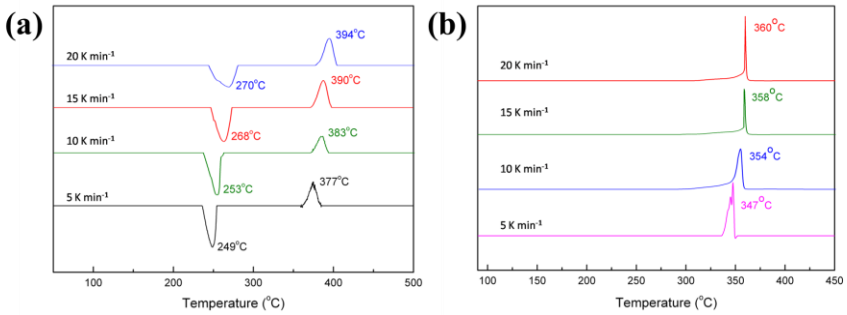

Figure 6: DSC curves for 2 (a) and 3 (b) at the heating rate of 5, 10, 15, 20 K min^{-1}.

To obtain the non-isothermal decomposition properties such as apparent activation energy E_a and pre-exponential constant A after the exothermic decomposition reaction, three multiple heating methods (*Kissinger*'s, *Ozawa*'s, and *Starink*'s methods [10-12]) were employed.

$$\ln\frac{\beta}{T_p^m} = -\frac{C_1 E_a}{RT_p} + C_2 \quad (1)$$

Here, β is heating rate (K min^{-1}), T_p is the decomposition peak (℃), E_a is the apparent activation

energy (kJ mol^{-1}), C_1 and C_2 are constant taken from the references. The calculation results are summarized in Table 1.

Table 1: The peak temperatures of the exothermal peaks at different heating rates and the chemical reaction kinetic parameters.

Heating rates β (K min^{-1})	T_p(℃)	Kinetic parameters	Kissinger's method	Ozawa's method	Starink's method
Comp. 2					
5	377	E(kJ mol^{-1})	275.07	272.90	274.68
10	383	ln(A) (s^{-1})	49.95	—	—
15	390	R	-0.9624	-0.9670	-0.9612
20	394				
Comp. 3					
5	347	E(kJ mol^{-1})	319.89	315.72	318.71
10	354	ln(A) (s^{-1})	61.34	—	—
15	358	R	-0.9939	-0.9938	-0.9939
20	360				

The self-accelerating decomposition temperature (T_{SADT}) and critical temperature of thermal explosion (T_b) were obtained by Equation (3) and Equation (4), respectively. [13,14] The results show that T_{SADT} and T_b of compound 2 are 370.0 ℃ and 383.0 ℃ respectively, and T_{SADT} and T_b of compound 3 are 337.5 ℃ and 347.5 ℃ respectively. The calculation results are summarized in Table 2. They are all higher than 1,3,5-trinitroperhydro-1,3,5-triazine (RDX), while slightly lower than octahydro-1,3,5,7-tetranitro-1,3,5,7-tetrazocine (HMX), indicating that the referenced compound possesses splendid thermal stability.

$$T_p = T_{p0} + b\beta_i + c\beta_i^2 \tag{2}$$

$$T_{SADT} = T_{p0} \tag{3}$$

Here, b and c are coefficients, β is the heating rate (K min^{-1}).

$$T_b = (E_a - \sqrt{E_a^2 - 4E_aRT_{p0}})/2R \tag{4}$$

Table 2: The self-accelerating decomposition temperature (T_{SADT}) and critical temperature of thermal explosion (T_b) for the referenced compound comparing with other commercial explosives.

	2	3	RDX[14]	NTO[13]	Tetryl[14]	HMX[14]
T_{SADT}[℃]	370.0	337.5	195.0	237.4	169.2	261.1
T_b[℃]	383.0	347.5	208.9	247.8	178.9	267.8

The entropy of activation ($\Delta S^{\neq}$), enthalpy of activation ($\Delta H^{\neq}$), and Gibbs free energy of activation ($\Delta G^{\neq}$) at T_{p0} can be obtained by applying the Equations (5)−(7). For compound 2, $\Delta H^{\neq}$ and $\Delta G^{\neq}$ of the reaction and the critical temperature of thermal explosion are calculated as follows: $\Delta S^{\neq}$=-218.79 J K^{-1} mol^{-1}, $\Delta H^{\neq}$=269.72 kJ mol^{-1}, and $\Delta G^{\neq}$=410.44 kJ mol^{-1}. For compound 3, $\Delta S^{\neq}$=-216.65 J K^{-1} mol^{-1}, $\Delta H^{\neq}$=219.18 kJ mol^{-1}, and $\Delta G^{\neq}$=447.11 kJ mol^{-1}.

$$A = \frac{k_B T}{h} e^{\Delta S^{\neq}/R} \tag{5}$$

$$\Delta H^{\neq} = E - RT \tag{6}$$

$$\Delta G^{\neq} = \Delta H^{\neq} - T\Delta S^{\neq} \tag{7}$$

Here, k_B is the Boltzmann constant and h is the Planck constant, $T=T_{p0}$, $E_a=E_k$ and $A=A_K$ (adopted from Kissinger's method).

3.5 Heat of formation and energetic performance

The heat of formation (HOF) of two energetic salts were predicted using density functional theory (DFT) method by Guassian 09 package. [15] The heats of formation (HOFs) for cation and anion of compound 2 were computed using isodesmic reaction (Scheme 2) at B3LYP/6-311G(d,p) level.

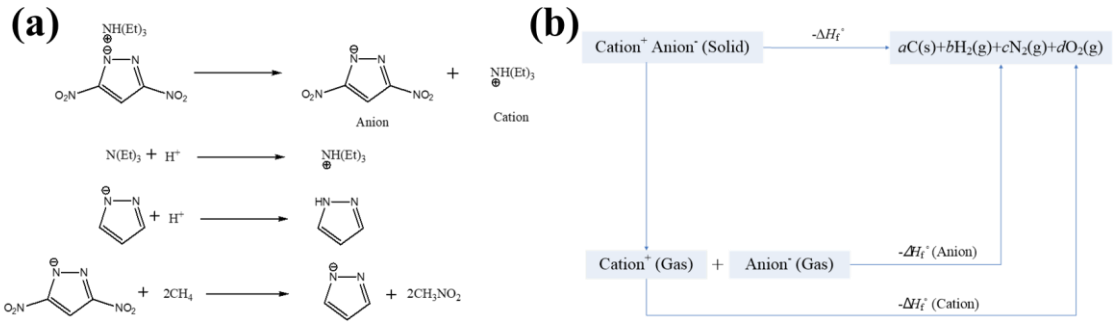

Scheme 2: Isodesmic reactions for anion and cation of $[DNP]NH(Et)_3$ (a) and Born-Habor Cycle for predicting the heat of formation of the energetic salts (b).

Based on a Born-Haber energy cycle, the solid HOF of organic energetic salt $[DNP]NH(Et)_3$ can be simplified as the following equation: [16]

$$\Delta H_f^o(ionicsalt,298K) = \Delta H_f^o(cation,298K) + \Delta H_f^o(anion,298K) - \Delta H_L \quad (8)$$

Where ΔH_L is the lattice energy of the salts that can be predicted by the following formula suggested by H. D. B. Jenkins et al.: [17]

$$\Delta H_L = U_{POT} + [p((n_M/2-2)+q(n_x/2-2)]RT \quad (9)$$

Where n_m and n_x depend on the numbers of the ions M_{p+} and X_{q-} respectively, which are equal to 3 for monatomic ions, 5 for linear polyatomic ions, and 6 for nonlinear polyatomic ions. The equation for lattice potential energy U_{POT} is shown as follows:

$$U_{POT} = \gamma(\frac{\rho}{M})^{1/3} + \delta \quad (10)$$

Here, ρ is the density and M is the formula mass of the ionic materials. For 1:1 (charge ratio) salts, the coefficients γ and δ are 1981.2 KJ mol^{-1} cm^{-1} and 103.8 kJ mol^{-1}, respectively. For 1:2 salts, the coefficients γ and δ are 8375.6 kJ mol^{-1} cm^{-1} and -178.8 kJ mol^{-1}, respectively.

HOF for coordination compound 3 was calcualted at Lanl2dz level using the atomization method (shown in Scheme 3) due to the exist of metal atoms.[18]

$$\begin{array}{ccc} aC + bH + cN + dO + eCu & \xrightarrow{\Delta H_f^0(M,298K)} & M \\ \downarrow \sum_{atom} x(H_X^0(0K) - H_X^0(298K)) & & H_M^0(298K) - H_M^0(0K) \uparrow \\ aC^0 + bH^0 + cN^0 + dO^0 + eCu^0 & \xrightarrow{\Delta H_f^0(M,0K)} & M^0 \end{array}$$

Scheme 3: The atomization method.

4. Conclusion

In this study, two novel energetic materials based on 3, 5-dinitropyrazole (3, 5-DNP) (2 and 3) were synthesized and their structures were confirmed by X-ray diffraction for the first time. Hirshfeld analysis showed that they both presented strong hydrogen-bond intermolecular interactions as shown in dominating H ··H, O ··H and H ··O contacts. Moreover, thermal-dynamic performance were evaluated by non-isothermal kinetic methods based on the results of differential scanning calorimeter (DSC), indicating that the two energetic materials possess excellent thermal properties (2: T_m=251℃, T_d=377℃; 3 : T_d=350℃). For 2, the apparent activation energy (E_a) evaluated by *Kissinger*'s, *Ozawa*'s, and *Starink*'s methods are 275.07, 272.90 and 274.68 kJ·mol^{-1}, respectively. And for 3, E_a estimated by three methods are 319.89, 315.72 and 318.71 kJ·mol^{-1}, respectively. Remarkably, 2 and 3 possess excellent thermal stability since the exothermic temperatures of them exceed 300 ℃, which are superior to those of reported copper-based nitrogen-rich salts or coordination compounds. Considering these above, it is worthwile to further explore the electronic properties of metal complexes of the DNP based energetic frameworks.

Acknowledgement

We are grateful for the financial support from the National Natural Science Foundation of China (NSFC, Grant Nos. 22175160).

References

[1] Gao H. X., Shreeve J. M. (2011) Azole-based Energetic Salts. Chem. Rev. 111, 7377-7436.
[2] Zhang Y., Gao Z., Liu W., Liu G., Zhu M., Wu S., Yao W., Gao E. (2021) Synthesis of Copper-based Metal-organic Framework for Sensing Nitroaromatic Compounds. Inorg. Chem. Comm. 134, 109017
[3] Loubalová I., Kopel P. (2023) Coordination Compounds of Cu, Zn, and Ni with Dicarboxylic Acids and N Donor Ligands, and Their Biological Activity: A Review. Mol. 28, 1445.
[4] Zhang Y. Q., Parrish D. A., Shreeve J. M. (2012) 4-nitramino-3, 5-dinitropyrazole-based Energetic Salts. Chem. Eur. J. 18, 987–994.
[5] Zhang Y. Q., Parrish D. A., Shreeve J. M. (2012) Synthesis and Properties of 3, 4, 5-trinitropyrazole-1-ol and Its Energetic Salts. Chem. 22, 12659–12665.
[6] Yin P., Damon A. P., Jean'ne M. S. (2015) Energetic Multifunctionalized Nitraminopyrazoles and Their Ionic Derivatives: Ternary Hydrogen-bond Induced High Energy Density Materials. Chem. Soc. 137, 4778–4786.
[7] Drukenmüller I. E., Klapötke T. M., Morgenstern Y., Rusan M., Stierstorfer J. (2014) Metal Salts of Dinitro-, Trinitropyrazole, and Trinitroimidazole. Z. Anorg. Allg. Chem. 640, 2139–2148.
[8] Wang Y. L., Zhao F. Q., Xu K. Z., Ji Y. P., Yi J. H., Chen B., An T. (2013) Synthesis, Crystal Structure and Thermal Behavior of 4-amino-3, 5-dinitropyrazole Potassium Salt. Inorg. Chim. Acta, 405, 505–510.
[9] Habraken C. L., Janssen J. W. A. M. (1971) The Formation of 3-Nitropyrazoles. J. Org. Chem. 36, 3081–3084.
[10] Kissinger H. E. (1957) Reaction Kinetics in Differential Thermal Analysis. Anal. Chem. 29, 1702–1706.
[11] Ozawa T. (1965) A New Method of Analyzing Thermogravimetric Data. Bull. Chem. Soc. Jap. 38, 1881–1886.
[12] Boswell P. G. (1980) On the Calculation of Activation Energies using a Modified Kissinger Method J. Therm. Anal. Calorim. 18, 353–356.
[13] Zhang T. L., Hu R. Z., Xie Y., Li F. P. (1994) The Estimation of Critical Temperatures of Thermal Explosion for Energetic Materials using Non-isothermal DSC. Thermochim. Acta 244, 171–176.
[14] Pourmortazavi S. M., Nasrabadi M. R., Kohsari I., Hajimirsadeghi S. S. (2012) Non-isothermal Kinetic Studies on Thermal Decomposition of Energetic Materials. J. Therm. Anal. Calorim. 110, 857–863.
[15] Frisch M. J., Trucks G. W., Schlegel H. B., Scuseria G. E., Robb M. A., Cheeseman J. R., Scalmani G., Barone V., Mennucci B., Petersson G. A., Nakatsuji H., Caricato M., Li X., Hratchian H. P., Izmaylov A. F., Bloino J., Zheng G., Sonnenberg J. L., Hada M., Ehara M., Toyota K., Fukuda R., Hasegawa J., Ishida M., Nakajima T., Honda Y., Kitao O., Nakai H., Vreven T., Montgomery Jr J. A., Peralta J. E., Ogliaro F., Bearpark M., Heyd J. J., Brothers E., Kudin K. N., Staroverov V. N., Keith T., Kobayashi R., Normand J., Raghavachari K., Rendell A., Burant J. C., Iyengar S. S., Tomasi J., Cossi M., Rega N., Millam J. M., Klene M., Knox J. E., Cross J. B., Bakken V., Adamo C., Jaramillo J., Gomperts R., Stratmann R. E., Yazyev O., Austin A. J., Cammi R., Pomelli C., Ochterski J. W., Martin R. L., Morokuma K., Zakrzewski

V. G., Voth G. A., Salvador P., Dannenberg J. J., Dapprich S., Daniels A. D., Farkas O., Foresman J. B., Ortiz J. V., Cioslowski J., Fox D. J. (2010). Gaussian 09 D. 01, Gaussian Inc, Wallingford.
[16] Gutowski K. E., Rogers R. D., Dixon D. A. (2007) Accurate Thermochemical Properties for Energetic Materials Applications. II. Heats of Formation of Imidazolium-, 1, 2, 4-Triazolium-, and Tetrazolium-Based Energetic Salts from Isodesmic and Lattice Energy Calculations. J. Phys. Chem. B, 111, 4788–4800.
[17] Jenkins H. D. B. (2002) Lattice Potential Energy Estimation for Complex Ionic Salts from Density Measurements. Inorg. Chem. 41, 2364–2367.
[18] Ma Q., Jiang T., Zhang X., Fan G., Wang J., Huang J. (2015) Theoretical Investigations on 4, 4'5, 5'-tetranitro-2, 2'-1H, 1'H-2, 2'-biimidazole Derivatives as Potential Nitrogen-rich High Energy Materials. J. Phys. Org. Chem. 28, 31–39.